SH3P2 in complex with Cbl and Src

Iwona Szymkiewicz[a,b], Olivier Destaing[c], Pierre Jurdic[c], Ivan Dikic[a,b,*]

[a]*Institute of Biochemistry II, Goethe University Medical School, Theodor-Stern-Kai 7, 60590 Frankfurt, Germany*
[b]*Ludwig Institute for Cancer Research, Box 595, Husargatan 3, Uppsala S-75124, Sweden*
[c]*Ecole Normale Supérieure de Lyon, UMR 5665 CNRS/ENS/INRA 913, 46 allée d'Italie, 69364 Lyon Cedex 07, France*

Received 19 February 2004; revised 17 March 2004; accepted 25 March 2004

First published online 15 April 2004

Edited by Gianni Cesareni

Abstract In this report, we describe SH3P2, an SH3-domain containing protein, as a novel Cbl-interacting molecule that is a substrate of tyrosine kinase Src. We identified a specific polyproline motif of Cbl responsible for binding of SH3P2 and Src, and observed mutual sequestration of Src and SH3P2 from monomer Cbl molecules. In adherent cells, SH3P2 associated with Cbl and fibrilar actin and was localized at focal contacts in fibroblasts as well as at the apical part of podosome rings in differentiated osteoclasts. Our data implicate that SH3P2, a novel component of adhesion sites, is involved in Cbl and Src-mediated pathways.

Keywords: Actin; Cbl; Osteoclast; Podosome; SH3; Src

1. Introduction

The identification of the proto-oncogene Casitas B-lineage lymphoma (Cbl) has been a starting point for many exciting discoveries that led to better understanding of how various signaling pathways regulate biological responses in living cells [1]. Thanks to its complex structure Cbl associates with receptor and non-receptor tyrosine kinases, mediates their ubiquitination, and serves as a scaffolding molecule for many signaling proteins. Cbl is a major substrate for Src family of tyrosine kinases, and together with Pyk2 kinase has been shown to be important for Src-mediated migration and function of osteoclasts [2,3]. Osteoclasts are multinucleated cells that originate from monocyte-macrophage lineage and are responsible for degradation of bone matrix [4]. They develop highly dynamic adhesion structures called podosomes, which contain Cbl and Src, as well as actin-associated proteins [5,6]. $Cbl^{-/-}$ osteoclasts are less motile and have decreased ability to invade and resorb bone in vivo [7]. Moreover, expression of truncated forms of Cbl inhibits formation of lamellipodia and membrane ruffles [8].

Here, we show that SH3P2, a molecule composed of a short proline-rich region, an SH3 domain and three ankyrin repeats, functions as a novel Cbl-interacting partner in mammalian cells. This protein has been originally cloned as SH3P2 in a systematic screen for SH3-domain containing proteins from a mouse embryo λcDNA library [9]. Additionally, a human homolog has been cloned as osteoclast stimulating factor (OSF) and shown to indirectly stimulate formation and activity of osteoclasts [10]. We demonstrated that the SH3 domain of this molecule bound to a specific polyproline motif in Cbl proteins, characterized the interactions between Cbl, SH3P2 and Src that led to increased tyrosine phosphorylation of SH3P2, and visualized the localization of SH3P2 in focal contacts and podosomes.

2. Materials and methods

2.1. Plasmids and products

Myc-tagged pCMVPLI vector expressing full size human SH3P2 (OSF) was provided by Sakamuri Reddy. R499A mutation was introduced to HA-Cbl by PCR using QuickChange (Stratagene) protocol. c-Src constructs were kindly provided by Sara Courtneidge, Cbl mutants by Wallace Y. Langdon. In ΔLZ-Cbl, a STOP codon was introduced at the position 852. Anti-SH3P2 antibody was obtained from a rabbit immunized with the peptide CRTLSNAEDYLDD-EDSD. We used the following mouse monoclonal antibodies: anti-HA (12CA5, Boehringer Mannheim), anti-Myc (9E10) and anti-phosphotyrosine (PY99) from Santa Cruz, anti-v-Src (Ab-1, Oncogene), anti-FLAG (M2) and anti-vinculin (clone Vin-11-5) from Sigma. Rabbit polyclonal anti-Cbl antibody was described previously [11]. Goat polyclonal anti-GST antibody was from Pharmacia. FITC-conjugated phalloidin and mouse ascites fluid (clone AC-15) recognizing non-muscle β-actin were from Sigma. Nocodazole (Sigma) was used at 2 μM. Cytochalasin D (Calbiochem) was used as described in Section 3.

2.2. Yeast two-hybrid screen

The screen was performed essentially in accordance with the Matchmaker Two-Hybrid System 2 manual (Clontech) as described previously [11]. The Y190 yeast strain and bait plasmid pYTH9 were provided by Pontus Aspenström.

2.3. Cell culture, transfections and immunoprecipitations

NIH3T3, HeLa and RAW 264.7 cells were from ATCC (Manassas, VI). HEK293T cells were transiently transfected by calcium chloride method, and 30 h after transfection cells were lysed in 1% Triton X-100 buffer containing inhibitors of proteases and phosphatases, and processed with immunoprecipitation or GST-fusion binding followed by SDS–PAGE and Western blotting as previously described [12].

2.4. Culturing of osteoclasts

Spleen cells of 6–8 week old male mice OF1 were seeded at 2500 cells/mm^2 and were cultured for 8 days on coverslips in the differentiation medium containing α-MEM medium (Life Technologies, Carlsbad, CA), 10% of fetal calf serum (Hyclone), 20 ng/ml of M-CSF, and 20 ng/ml of soluble recombinant RANK-L.

2.5. Indirect immunofluorescence studies

NIH3T3 cells were fixed in 4% paraformaldehyde in PBS for 20 min, treated with NH_4Cl (50 mM, 10 min), permeabilized in Triton X-100 (0.2%, 10 min) and blocked in 4% fetal calf serum. Preparations were

* Corresponding author. Fax: +69-6301-5577.
E-mail address: dikic@biochem2.uni-frankfurt.de (I. Dikic).

0014-5793/$22.00
doi:10.1016/j.febslet.2004.03.100

stained with FITC- or TRITC-phalloidin (Sigma) and anti-SH3P2 antibody followed by incubation with TRITC- or FITC-anti-rabbit antibodies, respectively (DAKO, Denmark). Images were taken with digital camera from Zeiss microscope Axioplan 2. For confocal imaging of osteoclasts, the cells were processed as described [13] and imaged with a Zeiss LSM 510 using 63× Plan Neo Fluor objective. Coverslips were mounted in Prolong® Antifade (Molecular Probes). To prevent cross-contamination between fluorochromes, each channel was imaged sequentially using the multitrack recording module before merging.

3. Results

3.1. Identification of SH3P2 as a binding partner of Cbl

The cDNA encoding SH3P2 protein was present in two out of 11 double positive Cbl-binding clones in a yeast two-hybrid screen with the human fetal brain cDNA library. Two other clones contained adapter protein Nck, previously known to interact with Cbl [14]. Both SH3P2 clones encoded the first 114 out of 214 amino acids, that is the SH3 domain and a part of the first ankyrin repeat (Fig. 1A). This cDNA was used to transform yeast clones expressing Cbl or Cbl fragments, and the double transformants were subjected to the β-galactosidase liquid culture assay. Result presented in Fig. 1B shows that the proline-rich stretch of Cbl is required for binding to SH3P2. This observation was confirmed by affinity precipitation experiments in mammalian cells (Fig. 1C). In this and following experiments, we used a rabbit polyclonal anti-SH3P2 antibody that specifically recognizes a band of 28 kDa (Fig. 1D). When resolved in SDS–PAGE gel, the recombinant Myc-tagged SH3P2 has somewhat higher molecular mass than endogenous SH3P2 from HEK293T cells (Fig. 1D).

3.2. Characterizing of proline-rich motif in Cbl responsible for binding to SH3P2

In order to map the SH3P2 binding site within the proline-rich stretch of Cbl, lysates from HEK293T cells expressing carboxyl-terminal truncation constructs of Cbl were incubated with full size SH3P2–GST fusion protein. The binding was reduced in the case of 528-Cbl and was completely lost in the case of 480-Cbl (Fig. 2A). The same pattern was obtained when the isolated SH3 domain of SH3P2 or Src fused to GST was used (not shown and Fig. 2A). The critical fragment in Cbl (residues 480–528) contains PPVPPR sequence that has been identified as SH3P2 ligand [9] and is a consensus site for binding of SH3 domain of Src [15]. This sequence is conserved among all mammalian Cbl members, Cbl, Cbl-b and Cbl-3, all of which associated with SH3P2 in GST-binding assay (not

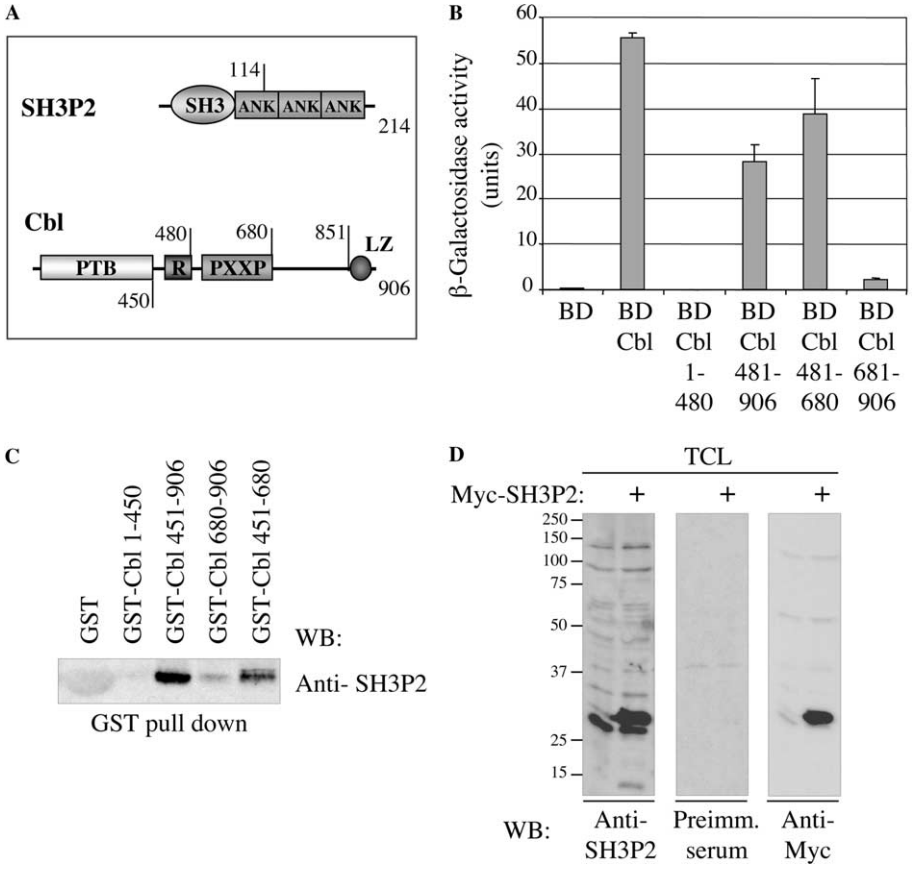

Fig. 1. SH3P2 binds to proline-rich domain of Cbl. (A) Structure representation of SH3P2 and Cbl. SH3, Src homology 3; ANK, ankyrin repeats; PTB, phosphotyrosine binding domain; R, RING finger; PXXP proline-rich sequences; LZ, leucine zipper. (B) Liquid culture assay using ONPG as substrate was used to calculate β-galactosidase activity in yeast. Yeast clones expressing Cbl or Cbl domains as fusion proteins with GAL4-DNA BD were transformed with SH3P2 (amino acids 1–114) fused to GAL4-activation domain. (C) Lysates from HEK293T cells transiently transfected with SH3P2 were incubated with equal amounts of GST or indicated GST fusion proteins. (D) Equal amounts of total cell lysates from HEK293T mock-transfected or overexpressing Myc-SH3P2 were probed with anti-SH3P2 serum or serum from the same rabbit prior to immunization (preimmune serum). After stripping, anti-Myc blot was performed to visualize the protein level.

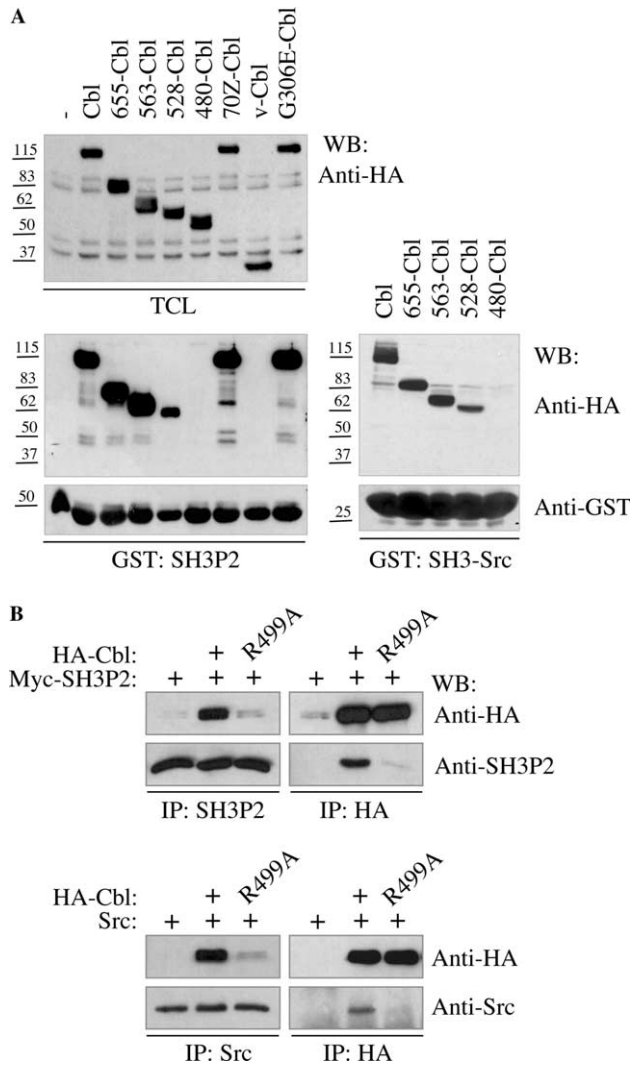

Fig. 2. Common motif in Cbl binds to SH3 domains of SH3P2 and Src. (A) Lysates from HEK293T cells overexpressing the indicated carboxyl-terminal deletion constructs of Cbl were incubated with either GST-conjugated SH3P2 or SH3 domain of Src. Upper panel: total cell lysates, lower panel: protein complexes binding to GST-fusion proteins. (B) Lysates from HEK293T cell transiently transfected with Cbl or R499A-Cbl together with SH3P2 or Src were immunoprecipitated and blotted as indicated.

shown). R499A-Cbl, which mutated the critical arginine in the PPVPPR motif, did not co-precipitate SH3P2 nor Src (Fig. 2B). Thus, we concluded that SH3 domains of both proteins recognize the same polyproline motif in Cbl.

3.3. Formation of SH3P2–Cbl–Src complexes

A previous report about SH3P2 (OSF) suggested that Src directly associates with SH3P2 [10], but despite all our attempts we could not demonstrate the binding between the two proteins. However, we observed that SH3P2 co-precipitates with c-Src in the presence of overexpressed Cbl (Fig. 3A). It is worth noting that the SH3P2 immunoprecipitates from Src-expressing cells contained a number of phosphorylated proteins, whose identity remains to be determined. Moreover, we showed that SH3P2 is a substrate for Src-mediated tyrosine phosphorylation in transiently transfected HEK293T cells (Fig. 3A). Endogenous SH3P2 was also phosphorylated in v-Src transformed fibroblasts (data not shown). Markedly, overexpression of Cbl increased the level of SH3P2 phosphorylation by c-Src (Fig. 3A).

E3 activity of Cbl results in ubiquitination and degradation of Src [16], and in order to stabilize the Cbl–Src complex we used an ubiquitination-deficient Cbl mutant (70Z-Cbl). As expected, the binding between Src and 70Z-Cbl was stronger than in the case of Cbl (Fig. 3B, bottom panel). Also, more SH3P2 was phosporylated in cells expressing 70Z-Cbl in comparison to cells expressing wild type Cbl (Fig. 3B, middle panel). Interestingly, we could see that both Cbl proteins are more phosphorylated by and associate stronger with c-Src in the absence of overexpressed SH3P2 (Fig. 3B). This suggested that SH3P2 competes with c-Src for binding to Cbl.

Dimerization of Cbl molecules could explain the seemingly contradictory observations of binding competition on the one hand and triple protein complex formation on the other. While the expression of full size Cbl enabled the complex formation between SH3P2 and Src, the deletion of carboxyl terminal LZ domain of Cbl, which normally mediates homodimerization of Cbl molecules [17], almost completely abrogated this effect (Fig. 3C, left panel). Notably, both SH3P2 and Src associate with ΔLZ-Cbl and Cbl to the same degree (Fig. 3C, right panel). The detectable weak band of Src complexed with GST-SH3P2 and ΔLZ-Cbl may be due to oligomerization of high amounts of mutant Cbl via other proteins (i.e., CIN85) that are able to bind and cluster Cbl molecules independently of the LZ domain [11,18]. Based on the results shown in Figs. 2 and 3, we propose a hypothesis where SH3P2 and Src in a mutually exclusive manner associate with individual Cbl molecules, that in turn by forming oligomers can facilitate the triple protein complex formation and phosphorylation of SH3P2 (Fig. 3D).

3.4. SH3P2 localization to actin structures

As shown in Fig. 4A, majority of SH3P2 was localized in the nuclear and peri-nuclear region, but it was also found in distinct areas at the periphery of NIH3T3 fibroblasts. In freshly plated cells, these areas co-localized with actin and were starting points for bunches of filamentous actin, which is a characteristic of focal complexes and microspikes in lamellipodia (Fig. 4A, upper panel) [19,20]. In cells attached for 24 h, SH3P2 was localized along the ends of stress fibers, in the areas close to the cell membrane (Fig. 4A, lower panel). In order to check if SH3P2 interactions are dependent on intact actin cytoskeleton, we treated HeLa cells with cytochalasin D, known to induce disassembly of F-actin [21]. As shown in Fig. 4B, in untreated cells SH3P2 associated with actin, while treatment with 3 and 10 μM cytochalasin D decreased the amount of actin associated with SH3P2. Removing the polymerization-blocking agent followed by 1-h incubation in normal media reconstituted the initial level of SH3P2–actin complex (Fig. 4B). Cytochalasin D treatment did not affect the Cbl–SH3P2 interaction. When the same amount of lysates was immunoprecipitated with anti-Cbl antibodies, we could not detect actin or SH3P2 in the precipitates (Fig. 4B), suggesting that only small fraction of Cbl may be involved in binding to SH3P2, and confirming the specificity of SH3P2–actin association.

3.5. SH3P2 localizes to podosomes in osteoclasts

In the light of previous implications of SH3P2 in osteoclast function, we analyzed the localization of this protein in

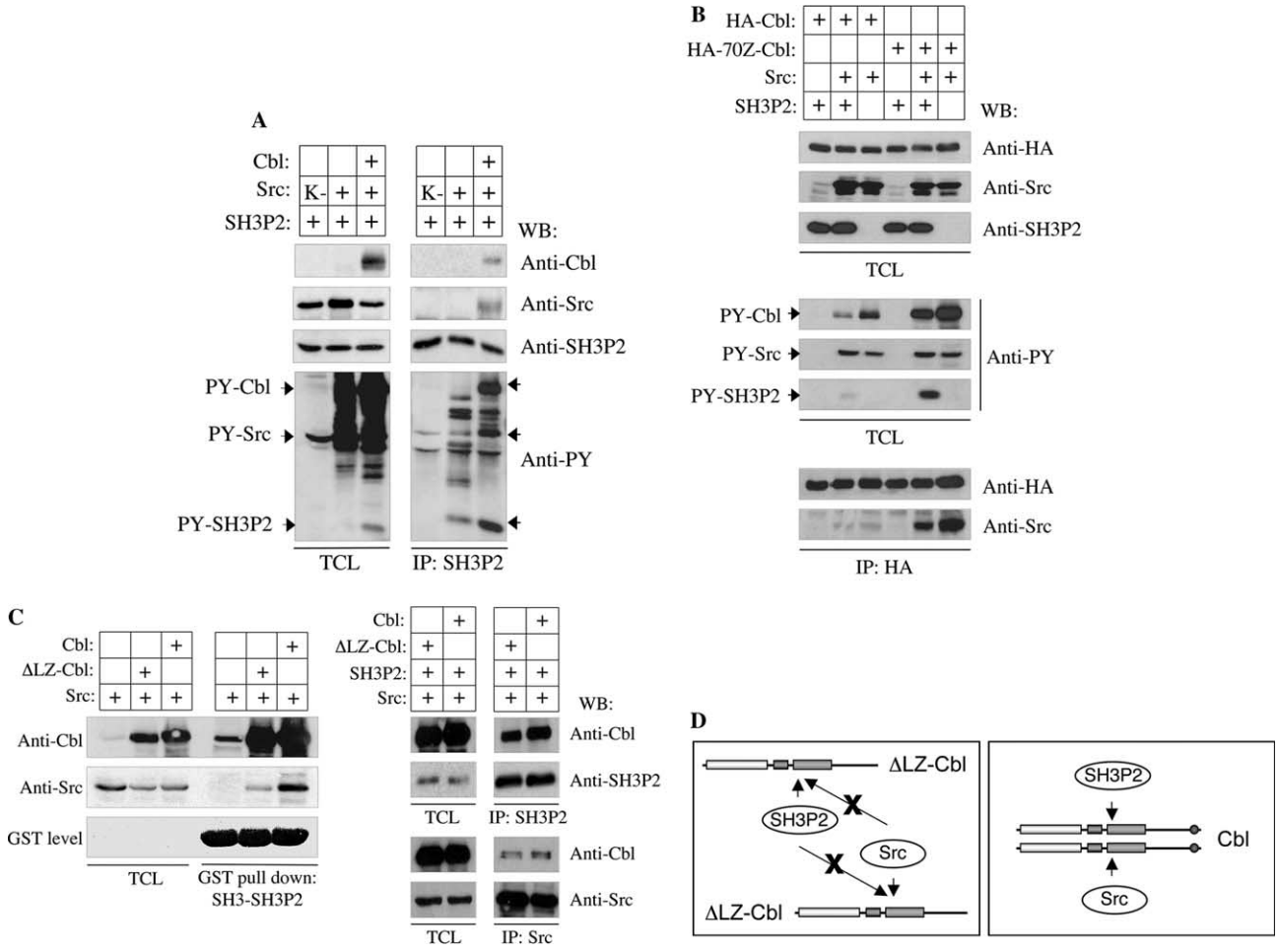

Fig. 3. The SH3P2–Cbl–Src complex. (A) HEK293T cells were transfected with SH3P2, c-Src, c-Src kinase-inactive (K−), and Cbl as indicated. Protein expression is shown in TCL panel. Protein complexes associated with SH3P2 are shown in the right panel. The nitrocellulose membranes were first probed with an anti-phosphotyrosine antibody (PY) and subsequently stripped and re-probed with indicated antibodies. (B) HEK293T were transiently transfected with the indicated cDNA constructs. Protein levels and phosphorylation pattern in total cell lysates (TCL) are shown in the upper and middle panels, respectively. Amount of c-Src associated with Cbl proteins is shown in the immunoprecipitates with anti-HA antibody (bottom panel). (C) Lysates from HEK293T cells expressing indicated cDNAs were incubated with GST fusion protein of SH3P2 and the bound proteins are shown in the left panel. Immunoprecipitation experiment in cells overexpressing SH3P2, Src and either ΔLZ-Cbl or Cbl is shown in the right panel. (D) Model of interactions within the SH3P2–Cbl–Src protein complex. Src and SH3P2 compete for binding to Cbl, and dimerization of full size Cbl, impaired in the case of ΔLZ-Cbl, facilitates complex formation between all three molecules.

osteoclasts. In differentiated osteoclasts, SH3P2 was present in the multiple nuclei and was also localized around podosomes at the peripheral belt (Fig. 5A). Upon treatment with nocodazole, which depolymerizes microtubules necessary for podosome distribution [22], SH3P2 remained associated with individual podosomes even when the peripheral actin belt was lost (data not shown). Vertical confocal sectioning of the centers of individual podosomes revealed that SH3P2 is localized preferentially in their apical tips, that is the part facing the inside of the cell (Fig. 5B, top panel). Cbl showed similar distribution (Fig. 5B, middle panel), while vinculin was found in the basal tip, oriented towards the plasma membrane (Fig. 5B, bottom panel). Accuracy of spatial resolution in the *z*-axis was confirmed by taking images of test beads and by using various fluorophores to detect the same marker (not shown). Cbl has been previously known to localize at the peripheral belt in osteoclasts [2], but the exact distribution in the context of individual podosome rings was not shown before.

4. Discussion

The recent identification of numerous Cbl interacting partners led to better understanding of Cbl's role in regulating diverse biological responses [1,23]. We found that a protein known as SH3P2 is a novel Cbl binder, which in not subjected to Cbl-mediated ubiquitination (data not shown), but can serve as adaptor in Cbl functions in actin cytoskeleton.

Characterization of the binding between SH3P2 and Cbl led us to identification of a polyproline motif in Cbl recognized by SH3 domains of SH3P2 and Src (Fig. 2). Although Src has been reported previously to bind to SH3P2 (OSF) in overexpression experiments [10], we could detect the SH3P2–Src association only in the presence of Cbl in the complex (Fig. 3A). Even though we cannot completely exclude the possibility of direct SH3P2–Src binding, our results rather indicate their indirect association through complex formation with Cbl molecules, and suggest concomitant and concentration-

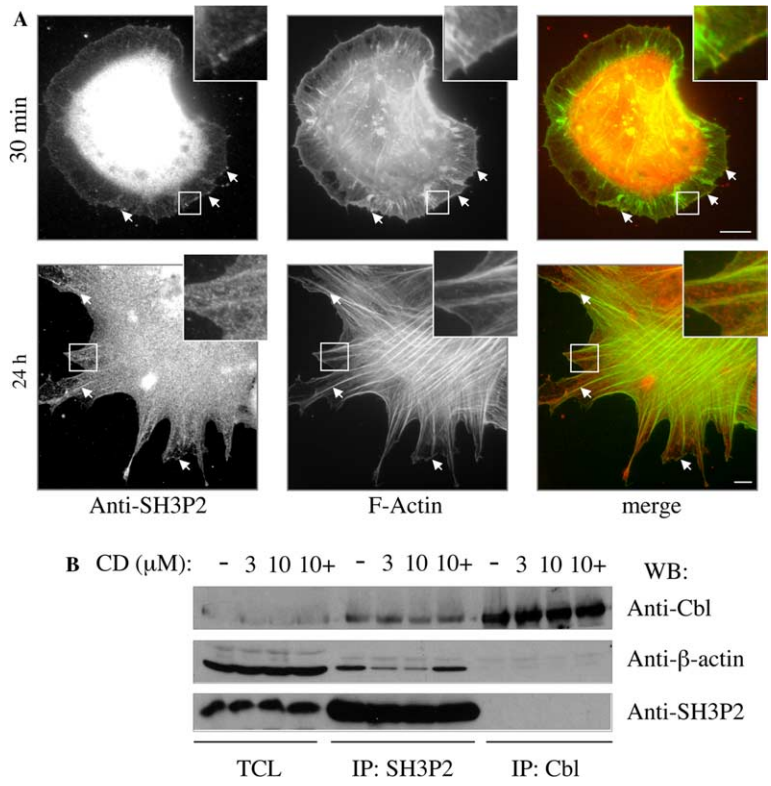

Fig. 4. SH3P2 colocalizes with actin in adherent fibroblasts. (A) NIH3T3 cells were allowed to attach to glass for 30 min or 24 h, fixed and stained for SH3P2 (red in merge) and F-actin (phalloidin, green in merge). Arrows point to selected places of colocalization; insets show details from cell periphery with SH3P2–actin overlap. Scale bars correspond to 10 μm. (B) HeLa cells were treated with cytochalasin D: 3 μM for 30 min (lane 3), 10 μM for 30 min (lane 10) or 10 μM for 30 min followed by wash and 1 h incubation in normal medium (lane 10+). Lysates were immunoprecipitated with anti-SH3P2 or anti-Cbl antibodies and blotted as indicated. TCL, total cell lysates.

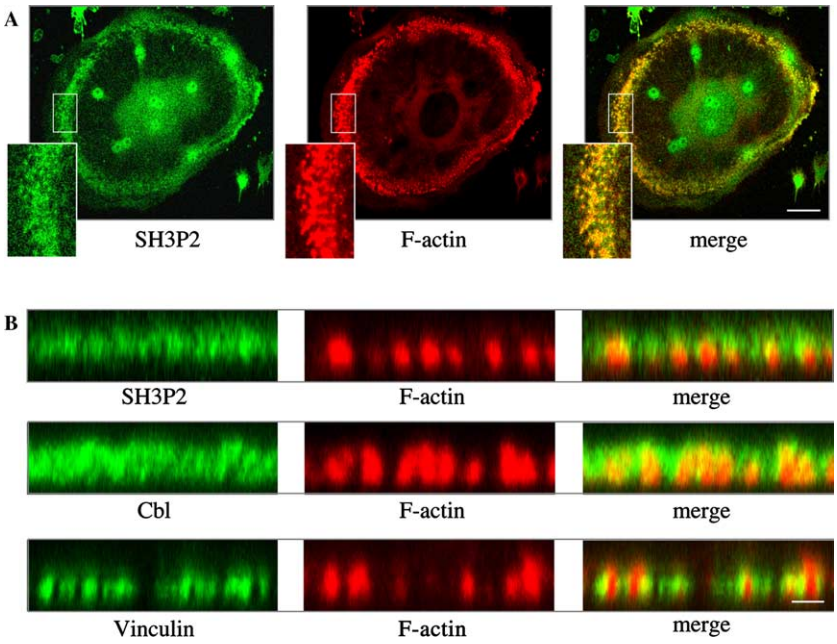

Fig. 5. Distribution of SH3P2 in osteoclasts. (A) Murine RAW 264.7 cells were differentiated in vitro as described in Section 2. The merged picture of SH3P2 and F-actin (phalloidin) is shown on the right. Scale bar, 20 μm. Enlarged image of the selected area of the podosome belt is shown in the left bottom corner of each picture. (B) Zoom on podosomes scanned in the *z*-axis. The bottom of each image corresponds to the substratum underneath cells. Scale bar, 2 μm.

dependent competition between SH3P2 and c-Src for binding to Cbl (Fig. 4).

SH3P2 was found in a complex with F-actin (Fig. 4B) and co-localized with dynamic actin filaments (Fig. 4A). In addition, we observed overlapping SH3P2 and vinculin distribution in elongated focal contacts in fibroblasts (not shown). SH3P2 was not binding to muscle F-actin in the actin precipitation assay (not shown), so the interaction is indirect, and is probably mediated via the ankyrin repeats of SH3P2 (our unpublished data).

Particular significance of Cbl and Src proteins has been demonstrated in osteoclasts, where Cbl acts downstream of c-Src in a signaling pathway required for bone resorption [3]. In osteoclasts, c-Src is associated with the ruffled border and co-localizes with Cbl in vesicular structures [3,24]. We demonstrated that SH3P2 together with Cbl is specifically distributed around individual podosomes of osteoclasts. Unlike integrin-associated proteins that localize to the distal side of podosome, both SH3P2 and Cbl were found in the apical part (Fig. 5B), which may suggest their role in downstream signaling rather than in assembling of the adhesion complexes.

Importantly, our observations suggest dynamic and locally regulated interaction and differential phosphorylation within the triple protein complex. According to our hypothesis, SH3P2 is constitutively associated with the Cbl pool localized at the cell-substratum adhesion sites. Activation of integrins or growth factor receptors induces Src-mediated phosphorylation of Cbl, while opening of Src structure and enhanced binding of Src to Cbl can result in phosphorylation of SH3P2 and its dissociation from Cbl. In order to further elucidate the SH3P2 role in the context of cell physiology, we are currently searching for other SH3P2 binding partners and are undertaking the gene targeting approach to analyze phenotypes of SH3P2 deficient cells.

Acknowledgements: We thank S. Reddy, S. Courtneidge, and P. Aspenström for providing reagents used in this study. We are grateful to L. Hajkova for helpful suggestions and critical reading of the manuscript. This work has been supported in part by grants from Swedish Research Council (to I.S.), charity funds from Association pour la recherche contre le cancer (ARC and Ligue contre le cancer (comité du Rhône)) (to P.J.), and the Swedish Strategic Funds and the Boehringer Ingelheim Foundation (to I.D.).

References

[1] Dikic, I., Szymkiewicz, I. and Soubeyran, P. (2003) Cell. Mol. Life Sci. 60, 1805–1827.
[2] Sanjay, A. et al. (2001) J. Cell Biol. 152, 181–195.
[3] Tanaka, S., Amling, M., Neff, L., Peyman, A., Uhlmann, E., Levy, J.B. and Baron, R. (1996) Nature 383, 528–531.
[4] Väänänen, H.K., Zhao, H., Mulari, M. and Halleen, J.M. (2000) J. Cell Sci. 113, 377–381.
[5] Destaing, O., Saltel, F., Geminard, J.C., Jurdic, P. and Bard, F. (2003) Mol. Biol. Cell 14, 407–416.
[6] Ochoa, G.C. et al. (2000) J. Cell Biol. 150, 377–389.
[7] Chiusaroli, R., Sanjay, A., Henriksen, K., Engsig, M.T., Horne, W.C., Gu, H. and Baron, R. (2003) Dev. Biol. 261, 537–547.
[8] Scaife, R.M. and Langdon, W.Y. (2000) J. Cell Sci. 113 (Pt 2), 215–226.
[9] Sparks, A.B., Hoffman, N.G., McConnell, S.J., Fowlkes, D.M. and Kay, B.K. (1996) Nat. Biotechnol. 14, 741–744.
[10] Reddy, S., Devlin, R., Menaa, C., Nishimura, R., Choi, S.J., Dallas, M., Yoneda, T. and Roodman, G.D. (1998) J. Cell Physiol. 177, 636–645.
[11] Soubeyran, P., Kowanetz, K., Szymkiewicz, I., Langdon, W.Y. and Dikic, I. (2002) Nature 416, 183–187.
[12] Blaukat, A., Ivankovic-Dikic, I., Gronroos, E., Dolfi, F., Tokiwa, G., Vuori, K. and Dikic, I. (1999) J. Biol. Chem. 274, 14893–14901.
[13] Ory, S., Munari-Silem, Y., Fort, P. and Jurdic, P. (2000) J. Cell Sci. 113, 1177–1188.
[14] Rivero-Lezcano, O.M., Sameshima, J.H., Marcilla, A. and Robbins, K.C. (1994) J. Biol. Chem. 269, 17363–17366.
[15] Sparks, A.B., Rider, J.E., Hoffman, N.G., Fowlkes, D.M., Quillam, L.A. and Kay, B.K. (1996) Proc. Natl. Acad. Sci. USA 93, 1540–1544.
[16] Yokouchi, M., Kondo, T., Sanjay, A., Houghton, A., Yoshimura, A., Komiya, S., Zhang, H. and Baron, R. (2001) J. Biol. Chem. 276, 35185–35193.
[17] Bartkiewicz, M., Houghton, A. and Baron, R. (1999) J. Biol. Chem. 274, 30887–30895.
[18] Kowanetz, K. et al. (2003) J. Biol. Chem. 278, 39735–39746.
[19] Geiger, B., Bershadsky, A., Pankov, R. and Yamada, K.M. (2001) Nat. Rev. Mol. Cell Biol. 2, 793–805.
[20] Watanabe, N. and Mitchison, T.J. (2002) Science 295, 1083–1086.
[21] Schliwa, M. (1982) J. Cell Biol. 92, 79–91.
[22] Babb, S.G., Matsudaira, P., Sato, M., Correia, I. and Lim, S.S. (1997) Cell Motil. Cytoskel. 37, 308–325.
[23] Dikic, I. and Giordano, S. (2003) Curr. Opin. Cell Biol. 15, 128–135.
[24] Boyce, B.F., Yoneda, T., Lowe, C., Soriano, P. and Mundy, G.R. (1992) J. Clin. Invest. 90, 1622–1627.